Yuzuncu Yil University
Journal of Agricultural Sciences
(Yüzüncü Yıl Üniversitesi Tarım Bilimleri Dergisi)
https://dergipark.org.tr/en/pub/yyutbd

ISSN: 1308-7576 e-ISSN: 1308-7584

Research Article

Determination of the Relationship between Rice Suitability Classes and Satellite Images with Different Time Series for Yeşil Küre Farm Lands

Orhan DENGİZ[1], Mert DEDEOĞLU[*2], Nursaç Serda KAYA[3]

[1,3] Ondokuz Mayıs University, Agriculture Faculty, Soil Science and Plant Nutrition Department, 55139, Samsun, Turkey
[2]Selcuk University, Agriculture Faculty, Soil Science and Plant Nutrition, Department, 42100, Konya, Turkey

[1]https://orcid.org/ 0000-0002-0458-6016, [2]https://orcid.org/ 0000-0001-8611-3724, [3]https://orcid.org/ 0000-0001-9814-5651

*Corresponding author e-mail: mertdedeoglu@gmail.com

Article Info

Received: 11.05.2022
Accepted: 20.06.2022
Online published: 15.09.2022
DOI: 10.29133/yyutbd.1114636

Keywords

Land evaluation,
NDVI,
RE-OSAVI,
Rice

Abstract: In this study, rice land designated for agricultural land suitability indices belonging to the enterprise Yeşil Küre Farm Land with different time series Sentinel-2A satellite images calculated utilizing spectral vegetation index, which are Normalized Difference Vegetation Index and Red Edge Optimized Soil Adjusted Vegetation Index values by statistical comparison of the relationship between rice for monitoring and estimation of potential productivity is presented a different perspective. Firstly, according to the rice suitability assessment for the study area, the area of 5488.9 ha was determined to be suitable for rice cultivation at the S1 and S2 levels, whereas the area of 588.9 ha was determined to be unsuitable. In this study, it was determined that the most successful results for each land conformity class were obtained using the NDVI. In particular, it was determined that August received the highest r^2 value (NDVI; 0.8580 and RE-OSAVI; 0.8465) in both vegetation index models at the S1 level, and on the other hand, a higher r^2 value was obtained with NDVI.

To Cite: Dengiz, O, Dedeoğlu, M, Kaya, N S, 2022. Determination of the Relationship between Rice Suitability Classes and Satellite Images with Different Time Series for Yeşil Küre Farm Lands. *Yuzuncu Yil University Journal of Agricultural Sciences*, 32(3): 507-526.
DOI: https://doi.org/10.29133/yyutbd.1114636

1. Introduction

Soil is a limited and non-renewable natural resource for the needs of the increasing human population, as well as being the main element in meeting the nutritional and shelter needs of the terrestrial ecosystem (Blum, 2006). As a matter of fact, it is predicted that the world population will grow by 19.7% until 2050 and reach 9.6 billion. The increase in the world population and the increase in the demand for food that it will bring with it causes the intensification of agricultural activities and an increase in the pressure on the limited land resources (FAO, 2009; Liniger, et al., 2011; Dumanski and Peiretti, 2013). Therefore, food security, demand for energy and water, climate change, and biodiversity in relation to sustainable land use are among the important global problems of the 21st century (Lal, 2008; 2009; Jones, et al., 2009; Lichtfouse, et al., 2009). The continuity of the functionality of the ecosystem depends on using the soil in the best way to get high productivity (Lal, 2009; Walter and Stützel, 2009).

Determination of soil quality is the basis of common and reliable approaches in the evaluation of soil fertility (Mueller et al., 2010; Ahmed et al., 2016; Xue et al., 2019; Dengiz, 2020). Soil quality

is defined as the capacity of soil to perform its functions within the boundaries of natural or managed ecosystems (Larson and Pierce, 1991; Doran and Parkin, 1994; Karlen, et al., 1997). Soil quality, like air and water, has a profound impact on the health and productivity of a particular ecosystem and its associated environments. Soil fertility is also the basic elements of a high input-based agricultural production system. For this reason, it is essential to evaluate soil fertility with parametric approaches in a periodic process (Rogowski and Wolf, 1994; Dengiz and Sağlam, 2012; Askari et al., 2015).

Today, Geographic Information Systems (GIS) and Remote Sensing (RS) technologies are useful tools used in similar monitoring issues encountered in the agricultural sector. Saving time and providing reliable, cost-effective, and repetitive information are among the advantages of GIS and UA to the agricultural sector. GIS and UA technologies are used in many areas, such as monitoring plant development process, evaluation of soil quality, crop yield estimation, and spatial analysis required in modern agriculture. As a matter of fact, the use of visible near infrared (VNIR) spectroscopy and GIS technologies in the evaluation of soil fertility by integrating agricultural practices and expert opinions makes it practical and economical to monitor agricultural areas locally (Moran, et al., 1996; Malczewski, 2006; Vohland, et al., 2014; Askari, et al., 2015). For this purpose, spectral reflections at different wavelengths obtained from earth observation satellites have been used to determine measurable plant vegetation characteristics such as plant biomass and active photosynthetic radiation since the launch of the Landsat-1 satellite in 1972 and to monitor the phenological changes of plants (Jackson, 1986). However, developing spectral sensors and band combination techniques have brought along the concept of vegetation index and have been widely used in the evaluation of cultivars grown in large-scale areas (Shou, et al., 2007; Jia, et al., 2011; Savasli, et al., 2021). It is known that especially the red (Red), red edge (Red-Edge), and near infrared (NIR) bands of the electromagnetic spectrum play an active role in monitoring the agricultural ecosystem (Liu, et al., 2004). Indeed, the relevant spectral regions are closely related to plant biophysical variables (height, density, and percentage of coverage), and it is known that the ratio of near-infrared bands to red edge spectral bands provides a high correlation with crop development in different growth periods. Today, many spectral indices, defined as unitless radiometric measurements, have been developed to obtain information about the biophysical properties of green leafy plants. The working principle of vegetation indices is basically based on the presence of chlorophyll, which is directly related to green leaf area and plant biomass and its response to biotic/abiotic factors (Kokaly and Clark, 1999; Li, et al., 2015). For this purpose, Normalized Difference Vegetation Index (NDVI), Effective Leaf Area Index, Chlorophyll Absorption Index at Modified Reflection Rate (Red-Edge Modified Chlorophyll Absorption in Reflectance Index), Red Edge Optimized Soildable Vegetation Index Red-Edge Optimized Soil Adjusted Vegetation Index, Green Normalized Difference Vegetation Index, Green Normalized Difference Vegetation, Health Index and Leaf Area Index are used (Fitzgerald, et al., 2010; Bagheri, et al., 2012; Wójtowicz, et al., 2016; Demir and Başayiğit, 2021). However, while studies have shown that vegetation indices derived from multi-spectral satellite images give successful results in early yield estimations, similar spectral index approaches that can directly evaluate the yield potential of soils could not evolve with a pragmatic model due to the complex nature of soils (Barnes et al., 2000). For this reason, the vegetation indices of the plants grown in agricultural lands and the biomass ratios determined at varying levels provide an indirect benefit to the researchers in the evaluation of soil fertility. In this way, the productivity of the soil where strategically important crops based on crop yield are grown under an agricultural management can be estimated experimentally (Gupta, et al., 2003; Zand and Matinfar, 2012; Mezera, et al., 2017; Sharabiani, et al., 2019). As a matter of fact, the factors affecting plant spectral reflections and indices values may be due to differences in management practices, as well as related to soil fertility (Zhou, et al., 2018; Dedeoğlu, et al., 2020). With this study, it is aimed to establish the land suitability classes of rice lands of Yeşil Küre Agricultural Enterprise and to reveal the relationship between NDVI and RE-OSAVI vegetation index values produced from Sentinel-2A satellite images with different time series and rice land suitability classes.

2. Material and Methods

Yeşil Küre Agricultural Enterprise (Center) is located at the 40th km on the Samsun-Bafra highway and is between 249000-254000 East and 4599200 - 4602400 North (WGS84, Zone 37, UTM-m) coordinates. Total land asset is 9239.8 da. Düden, which is the other part of the operation area where

the Black Sea is located in the east, Bünyan Mountain in the south, and the Bafra Plain in the west and north, is adjacent to the western shore of Balık Lake in the Kızılırmak Delta.

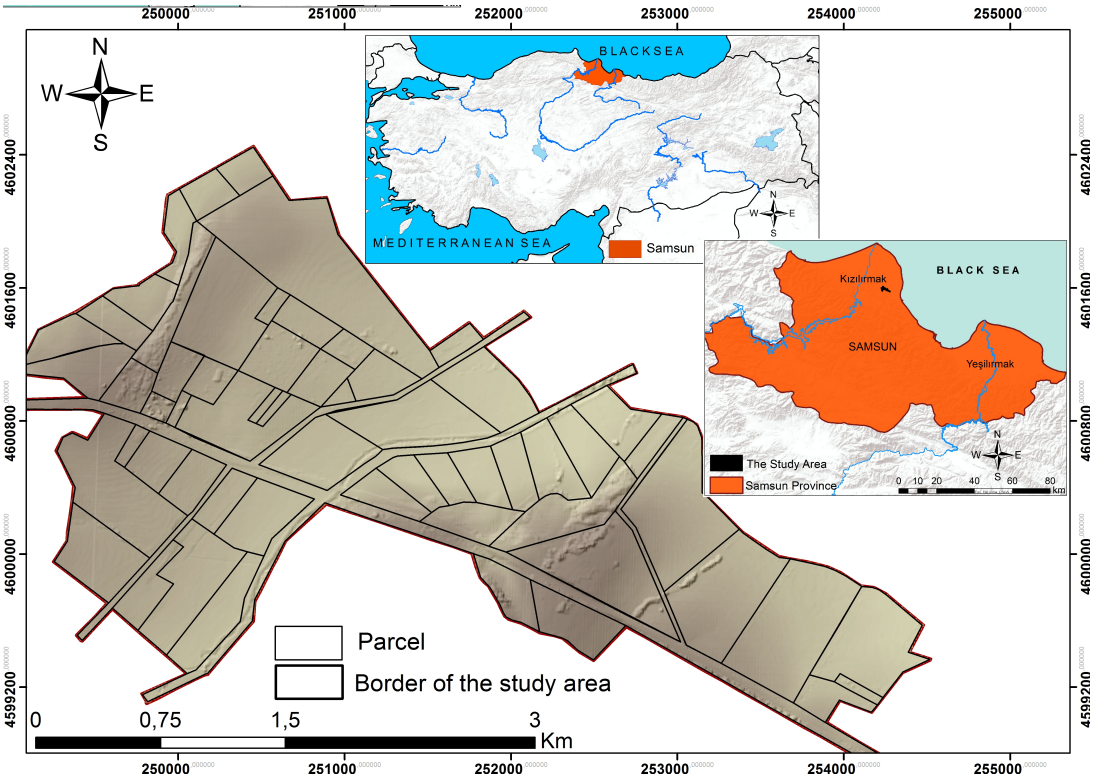

Figure 1. Location map of Yeşil Küre agricultural enterprise.

The height of the operation lands (Center and Düden) above sea level varies between 5 and 74 m. While the northwest and southeast parts of the land are areas where moderately steep and steep slopes are distributed in terms of slope, generally, the middle and northwest parts of the land constitute areas with 0-4%, nearly flat and mild slopes (Figure 2).

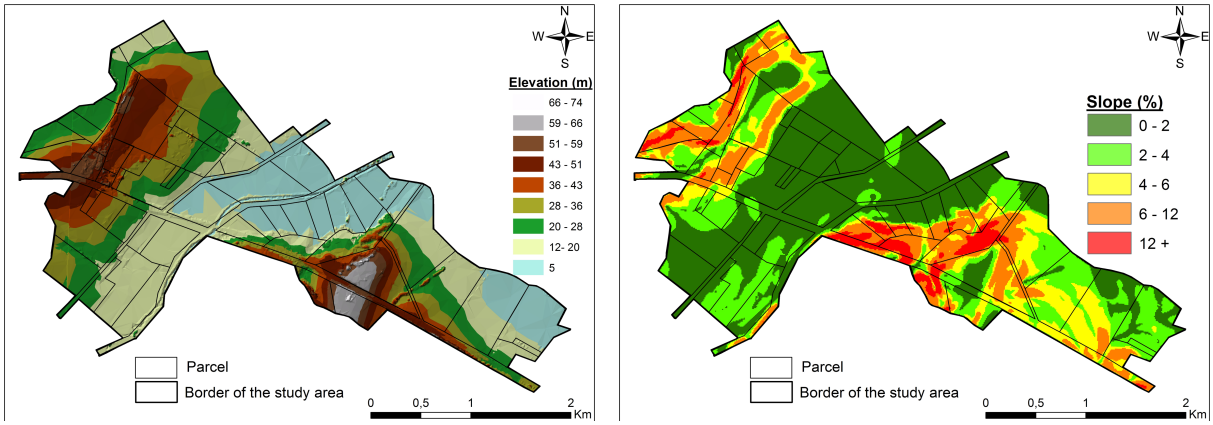

Figure 2. Elevation and slope map of the study area.

The widest coastal plains of the Black Sea Region are Çarşamba and Bafra plains. Yeşil Küre Agricultural Enterprise is also located on the Bafra Plain. The Black Sea climate, which is rainy in all seasons, cool in summers and warm in winters, is active on the coastline of the Black Sea Region. This effect of the climate extends to the inner parts depending on the landforms in the Central Black Sea Region. The annual average temperature of Yeşil Küre Agricultural Enterprise was 14.3˚C, the highest average air temperature was 18˚C and the lowest average temperature was 10.7˚C. The annual

precipitation average of the enterprise is around 710.0 mm. Snowfall in this region is less and does not last long. Snow does not stay for long in the coastal part. The coldest months in Bafra district are January, February and the hottest month is August.

The Bafra Plain, where the Yeşil Küre Agricultural Enterprise lands are located, is a wide delta plain formed by the rich alluvial soils brought by the Kızılırmak river. Bafra Plain is the largest plain of the Black Sea Region. Kızılırmak has formed many lakes near the sea. The area where the Agricultural Enterprise is located is covered by new Holocene alluvial deposits. In the central enterprise, there are high lands that emerged as a result of the erosion of these alluviums and carrying the eroded material (MTA, 1974). In addition, another series was added to the soil profiles in the updated study carried out in 2021 for the series classified as vertisol, mollisol, and entisol in the soil mapping study of the area carried out in 2005 by the General Directorate of Agricultural Enterprises, and the Yörükler series, which was classified as mollisol, was included in the entisol order due to losing its mollic feature as a result of intensive agricultural applications. (Figure 3).

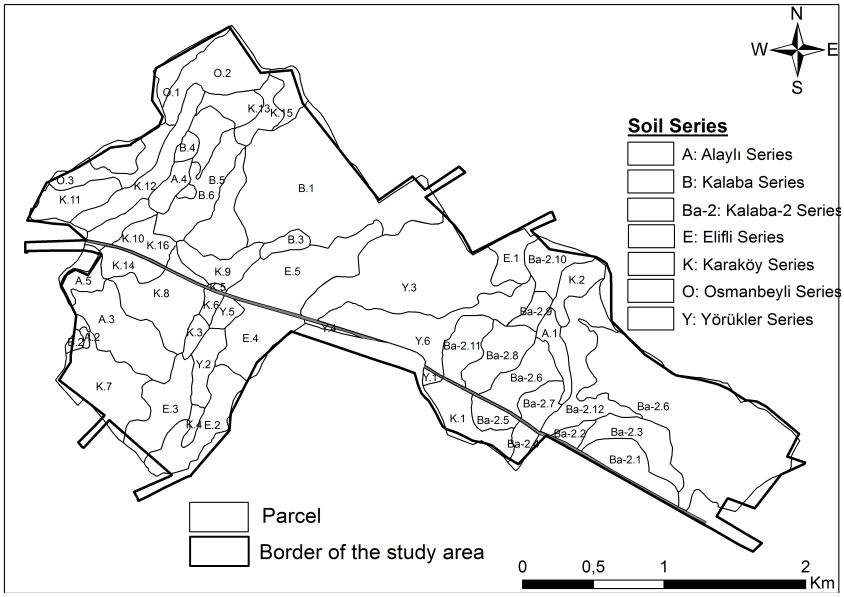

Figure 3. Updated soil map of the study area.

Almost all of the central part of the study area, called "Hara", has been cultured. Corn, wheat, alfalfa, and garlic are grown extensively. In addition, hazelnut and blackberry are planted. Rice farming is carried out in the farm area called Düden, located around Balık Lake in the Bafra delta. There are also oak, pine, poplar, maple, and elm trees, as well as ash, which are naturally found among dense rice fields. In Düden, natural living conditions prevail in the lower parts of the sea, where rice farming is not done. These regions are used as seasonal pastures by the local people. However, in periods when the rainfall is not heavy, cattle can be found in this region for grazing and sheltering.

Table 1. Characteristics of the Sentinel-2 satellite sensor

Band	Name	Wavelength (nm)	Band width (nm)	Spatial Resolution (m)
B1	**Coastal Aerosol**	443	20	60
B2	**Blue**	490	65	10
B3	**Green**	560	35	10
B4	**Red**	665	30	10
B5	**Vegetation Red-Edge**	705	15	20
B6	**Vegetation Red-Edge**	740	15	20
B7	**Vegetation Red-Edge**	783	20	20
B8	**Infrared**	842	115	10
B8A	**Vegetation Red-Edge**	865	20	20
B9	**Water vapor**	945	20	60
B10	**Cirrus**	1380	30	60
B11	**SWIR1**	1610	90	20
B12	**SWIR2**	2190	180	20

In this study, a total of 4 Sentinel-2 satellites images (with WGS84 datum) dated May, June, July and August 2021 of the Yeşil Küre Agricultural Enterprise lands on which various cultural plants are grown were used (Figure 4). Satellite images were obtained from the United States Geological Survey (USGS) open access center (https://earthexplorer.usgs.gov/). Multispectral Sentinel-2 satellite images have a spatial resolution of 10 m in 4 bands, 20 m in 6 bands, and 60 m in the other 3 bands (Table 1).

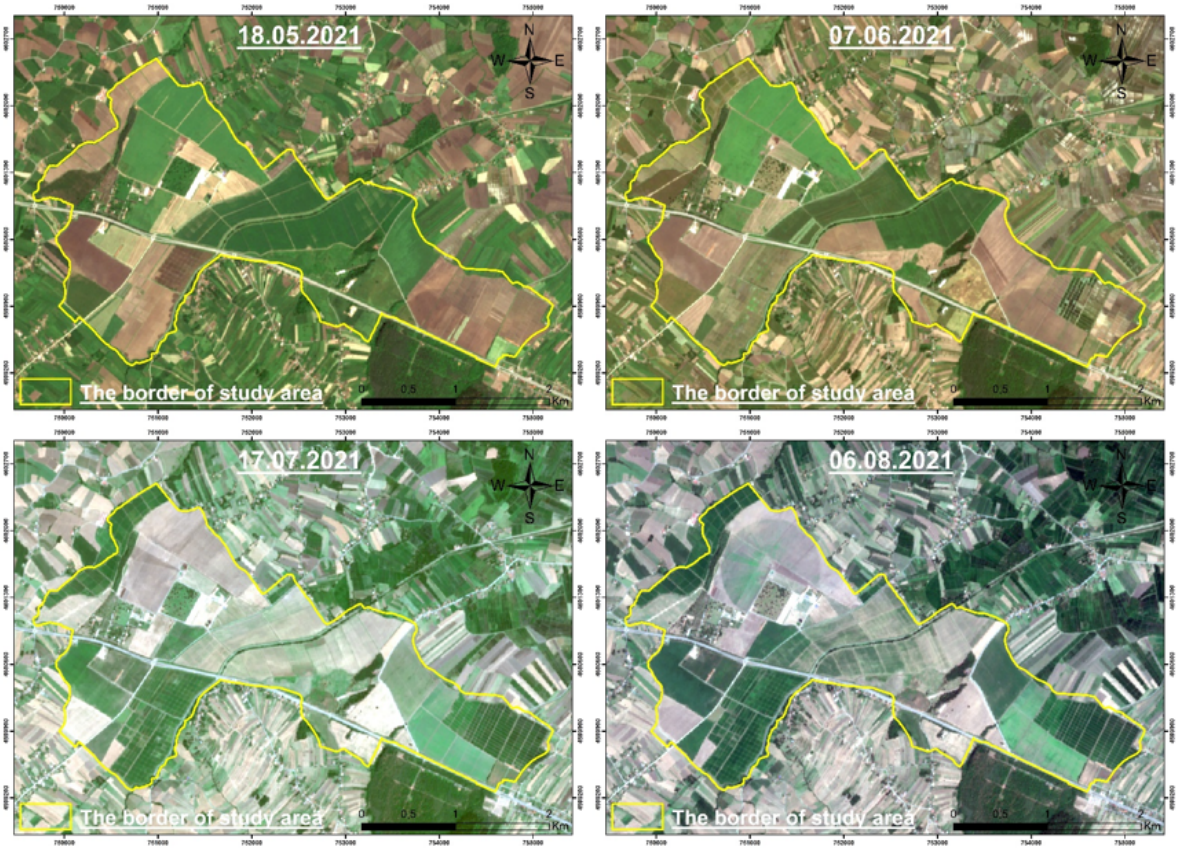

Figure 4. Sentenal-2 satellite images of different months.

2.1. Method

2.1.1. Creation of rice land suitability classes and index values

Soil series and their important phases were used as the mapping unit in the creation of the 1:25,000 scale basic soil map of the Yeşil Küre Agricultural Enterprise. Soil Survey Staff (1962) and Özbek et al., (1974) were used to classify important criteria such as depth, slope, salinity, alkalinity, drainage, and stoniness observed in the separation of soils into phases. Then, these criteria of the study area and topographic data were used to create the rice land suitability classes and index values. The determination of rice land suitability index values in terms of topographic and soil physico-chemical criteria has been handled by many researchers (FAO, 1983 and 1985; Sys et al., 1993; Yamada et al., 1995; Sönmez, 2003; Özcan, 2004; Mongkolsawat et al., 2002; Dengiz, 2013). These criteria used to determine the rice land suitability indices were obtained by multiplying the quality index value (SQI) (Equation 1) of the rice land soils belonging to each soil series with the nutrient availability index value (NAI) (Equation 2) and (Equation 3).

$$SQI: R * T * D * F * Y * P * G * S * K * H \quad (1)$$

R: Drainage, T: Texture, D: Depth, T: Topography, Y: Surface stony, P: Cream layer, G: Hydraulic conductivity, S: Salinity, K: Lime, H: Soil reaction.

$$NAI = N * P * K * Zn \quad (2)$$

NAI: Nutrient availability index.

$$LSC = NAI\ SQI \quad (3)$$

LSC: Land suitability class, NAI: Nutrient availability index, SQI*: Soil quality index.

Table 2. Rice suitability classes and index values

Statement	Suitability Classes	Index Value
Very suitable	S1	1.00-0.250
Moderate Suitable	S2	0.250-0.100
Low Suitable	S3	0.100-0.025
Not Suitable	N	< 0.025

2.1.2. Vegetation indexes

In this study, the vegetation indices of NDVI and RE-OSAVI, which are chlorophyll sensitive indices, were applied on the different time series Sentinel-2 satellite images of the rice fields of the Yeşil Küre Agricultural Enterprise by using the SNAP 8.0 tool and ArcGIS 10.7 environment. Information on both indexes is presented below.

2.1.2.1. Normalized difference vegetation index (NDVI)

There are many methods used in the identification of herbal product phenology. NDVI is the most widely used among these methods (Matton, et al., 2015). There have been many studies emphasizing the importance (Pettorelli et al., 2005a) of the role of satellite images in ecology, especially on the Normalized Difference Vegetation Index (NDVI) (Kerr and Ostrovsky, 2003; Damian, et al., 2019; Vorobiova and Chernov, 2017). As a matter of fact, Sahararini, et al. (2020) reported that the NDVI algorithm can be used as a base for processes such as image processing in Sentinel-2 satellite data, determination of rice phenology, estimation of rice harvest time. NDVI is used by many national and international organizations in many countries as an indicator of product yield. NDVI provides information with values ranging from -1 to +1 on subjects such as the spatial and temporal distribution of plant communities, plant biomass, CO_2 flows, pasture quality, and land degradation in various ecosystems (Salinas-Zavala et al., 2002; Al-Bakri et al., 2004; Pettorelli et al., 2005; Jiang et al., 2021).

NDVI values approaching -1 on the specified scale correspond to water bodies, while values approaching 0 indicate the presence of bare lands, rocky areas, sand, snow, or residential areas. NDVI values ranging from 0.2 to 0.4 correspond to bush or pasture areas, while this value approaching +1 indicates the presence of temperate regions, tropical rainforests, or areas with healthy and dense vegetation. With NDVI, it helps users in subjects such as the absorption of red wavelength energy within the visible region on the electromagnetic spectrum by the chlorophyll of the plant and the reflection of infrared (IR) energy by the plant cell structure, determination of biomass, and monitoring of changes in product development and production. By using NDVI in different time series satellite images, different growth periods of the plant, such as tillering, rooting, and harvesting, can be observed (Hufkens et al., 2019). In the Sentinel-2 satellite image, NDVI is calculated by using the red (B4) and infrared (B8) bands (Equation 4). The NDVI class values used in the estimation of the amount of product to be obtained from rice plants are given in Table 3.

$$NDVI = \frac{NIR - RED}{NIR + RED} \quad (4)$$

Table 3. NDVI values used in the definition of rice phenology (Pradipta, 2012).

NDVI values	Vegetation density	Age of Rice Plant (number of weeks after planting)
-0.096-0.036	No vegetation/bare/water	<3
0.036-0.240	Very low	3 - 4
0.240-0.456	low	4-6
0.456-0.652	Middle	6-8
0.652-0.884	high	8-13

2.1.2.2. Rededge optimized soil adjusted vegetation index (RE-OSAVI)

RE-OSAVI is an updated version of the Soil Vegetation Index (SAVI) family developed by Rondeaux et, al., (1996). The Optimized SAVI (OSAVI) model (RE-OSAVI) has been updated with the addition of the red edge (705 nm) band instead of the red band (670 nm) to minimize the effect of the submass on the red wavelength spectral reflections and make it more sensitive to the green field. It has been reported that this index can be used especially in periods when the vegetation density of plants is low (Wu et al., 2008). RE-OSAVI is calculated using the following formula (Equation 5).

$$\mathrm{RE-OSAVI} = (1 + 0.16) \times [(\mathrm{NIR} - \mathrm{REdge})/(\mathrm{NIR} + \mathrm{REdge} + 0.16)] \quad (5)$$

Vegetation indices (NDVI, RE-OSAVI) were calculated using the ESA-SNAP 8.0 tool in Sentinel-2 satellite images of the rice fields of the Yeşi Küre Farm Land.

2.1.3. Production of thematic maps and spatial statistical analysis in GIS environment

NDVI and RE-OSAVI vegetation index values were derived from each satellite image on a pixel basis, and maximum (S1), average (S2, N), and minimum (S3) NDVI and RE-OSAVI values were obtained for each rice suitability class. Thus, index values representing each parcel belonging to different rice land suitability classes were created. ArcGIS 10.7v was developed by ESRI (2010), for this purpose. Using the Zonal Statistics tool in the Spatial Analysis extension of the software, the index values reserved for different plots were extracted and transferred to MS Excel. Then, all indices' values were statistically compared with rice land suitability index (LSI) values, and regression relations (r^2) were determined.

3. Results and Discussion

3.1. Distribution of rice suitable areas

The areal and proportional distributions of rice suitability classes in the study area are given in Table 4, and its map is given in Figure 5. It was determined that 7205.5 da area, which is more than half of the study area (69.6%), is suitable for rice cultivation (S1 and S2), while 588.9 decares, which corresponds to 7.8% of the area, were found to be unsuitable for rice cultivation. In addition, depending on the limiting factor (slope, soil depth, texture, etc.) and grade of rice cultivation, less suitable (S3) classes cover 23.0% of the area.

Table 4. Spatial-proportional distributions of rice suitability classes

Statement	Suitability Classes	Area (da)	Ratio (%)
Suitable	S1	2964.4	37.6
Moderate Suitable	S2	2524.5	32.0
Low Suitable	S3	1816.3	23.0
Not Suitable	N	588.9	7.4
Total	-	7894.1	100.0

Areas that are not suitable for rice cultivation in the study area are generally the K12 and K11 mapping units of the Karaköy series, located in the northwest of the study area, and the B7, B8, B9, and B11 mapping units of the Kalaba series, which are distributed in the southeastern parts of the study area, especially the height and elevation in the slope grade. It has been determined that unsuitable areas are formed due to factors such as soil shallowness.

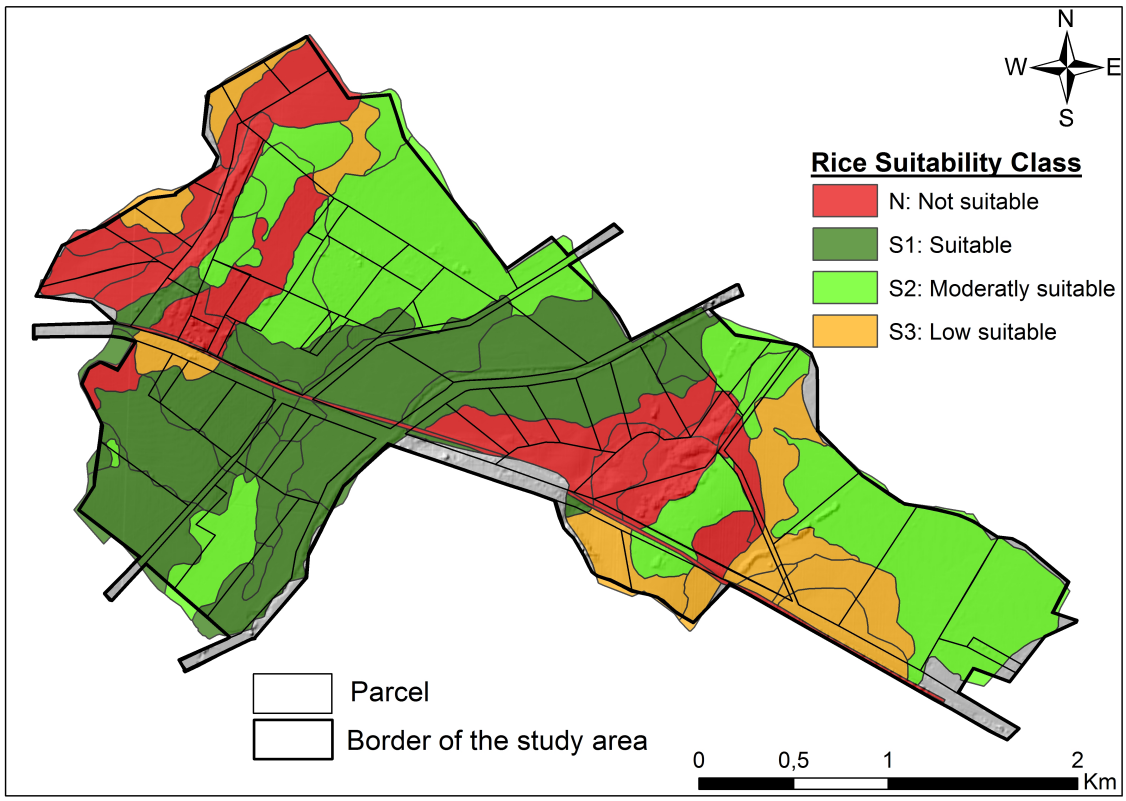

Figure 5. Rice suitability distribution map of the study area.

3.2. The relationship between rice suitability classes and vegetation indices

The land suitability index values for each land suitability class (S1, S2, S3, and N) of the rice fields obtained from the satellite images during May, June, July, and August dated May, June, July, and August of 2021, and the land suitability index values of the Sentinel-2A satellite images with different time series. The NDVI values and the r^2 values between which the statistical relationship was established are given in Table 5 and Figure 6, respectively. When the statistical relationship between the NDVI values obtained from the satellite image of May and the rice suitability index classes (S1, S2, S3, and N) is examined, the r^2 values are 0.7583, 0.8878, 0.8212, and 0.992, respectively; The r^2 values of the statistical relationship between the NDVI values obtained from the satellite image of June and the rice suitability index classes (S1, S2, S3, and N) were determined as 0.795, 0.873, 0.4725 and 0.9274, respectively.

In addition, the r^2 values of the statistical relationship between the NDVI values obtained from the July satellite image and the rice suitability index classes (S1, S2, S3, and N) were determined as 0.8396, 0.8833, 0.8879, and 0.9135, respectively, and finally, obtained from the August satellite image. When the statistical relationship between the obtained NDVI values and the rice suitability index classes (S1, S2, S3, and N) was examined, the r^2 values were found to be 0.858, 0.898, 0.8394, and 0.8924, respectively.

It should not be ignored that data variability may be caused by different cultural practices (fertilization, irrigation, soil cultivation, hoeing, etc.), such as the r^2 values of which the statistical relationship between the individual NDVI values of the land suitability classes and the ones belonging to the S3 suitability class are higher than the r^2 values of the S1 suitability class. (Dedeoğlu, et al., 2020).

Table 5. Each land suitability index values of rice fields and NDVI values of Sentinel-2A satellite images with different time series

Mapping Unit	Land Suitability Index	Land Suitability Class	NDVI Values			
			18.05.2021 Sentinel-2A	07.06.2021 Sentinel-2A	17.07.2021 Sentinel-2A	06.08.2021 Sentinel-2A
B11	0.02	N	0.6305	0.3091	0.2132	0.1530
B7	0.02	N	0.7319	0.5377	0.5690	0.4742
B8	0.016	N	0.6916	0.2862	0.4149	0.4987
B9	0.02	N	0.7359	0.7263	0.3275	0.3910
K11	0.016	N	0.5512	0.4934	0.3717	0.4185
K12	0.02	N	0.7368	0.5280	0.5277	0.4237
YOL	--	--	--	--	--	--
A1	0.4	S1	0.8119	0.8233	0.8135	0.8203
Ba.2	0.32	S1	0.7416	0.7217	0.6324	0.5041
Ba.4-A4	1	S1	0.6086	0.6348	0.7634	0.8094
Ba3	0.64	S1	0.8059	0.7391	0.6923	0.7842
E2	0.64	S1	0.5477	0.5507	0.6835	0.7711
E4-Y3	1	S1	0.7583	0.7677	0.7614	0.7795
E5	0.64	S1	0.7501	0.7662	0.7530	0.7753
K10	0.256	S1	0.7043	0.7114	0.8114	0.8093
K3	0.256	S1	0.7723	0.8009	0.8109	0.8050
K3	0.625	S1	0.7828	0.7541	0.8081	0.8037
K6	0.4	S1	0.8459	0.8108	0.7922	0.7317
K7	0.32	S1	0.7860	0.7860	0.7455	0.7968
K8	0.5	S1	0.7195	0.7766	0.7615	0.7950
K8	0.5	S1	0.8282	0.8011	0.7897	0.8043
K9	0.512	S1	0.8277	0.7542	0.7146	0.7198
Y1-E1	0.25	S1	0.8435	0.8053	0.7691	0.7305
Y2	0.4	S1	0.8481	0.8136	0.7547	0.7351
Y4-A3	0.205	S2	0.2462	0.3331	0.5227	0.6367
Y5	0.16	S2	0.4133	0.3386	0.2319	0.2064
A2	0.18	S2	0.6273	0.4220	0.2983	0.2493
A4	0.2	S2	0.5202	0.2388	0.5191	0.6134
A4	0.16	S2	0.7707	0.5536	0.2460	0.3673
A4	0.18	S2	0.7244	0.7342	0.2395	0.3238
B10	0.22	S2	0.7302	0.6552	0.1863	0.3435
B5-B9	0.16	S2	0.6897	0.5321	0.3012	0.3566
B6	0.25	S2	0.6195	0.5511	0.3192	0.3295
Ba.1	0.18	S2	0.7500	0.7136	0.1442	0.3505
Ba.4	0.2	S2	0.5989	0.5520	0.3741	0.4768
E3	0.14	S2	0.7540	0.7198	0.1325	0.4039
E3	0.25	S2	0.5630	0.5738	0.3178	0.3148
K2	0.128	S2	0.7534	0.7182	0.1519	0.3046
K2	0.1	S3	0.1545	0.1746	0.2079	0.1565
K2	0.08	S3	0.1216	0.1179	0.0786	0.0579
B1	0.08	S3	0.1430	0.1403	0.1470	0.1236
B2	0.054	S3	0.1237	0.1312	0.1880	0.1586
B3	0.042	S3	0.1402	0.1308	0.1027	0.1011
K1	0.05	S3	-0.0218	-0.2451	0.1350	0.1657
O1	0.051	S3	0.1344	0.1119	0.1129	0.1728
O2	0.09	S3	0.1067	0.1851	0.1123	0.1321
B12	0.05	S3	0.1492	0.1322	0.0876	0.0906

A*: Alaylı, B*: Kalaba, E*: Elifli, K*: Karaköy, O*: Osmanbeyli, Y*: Yörükler.

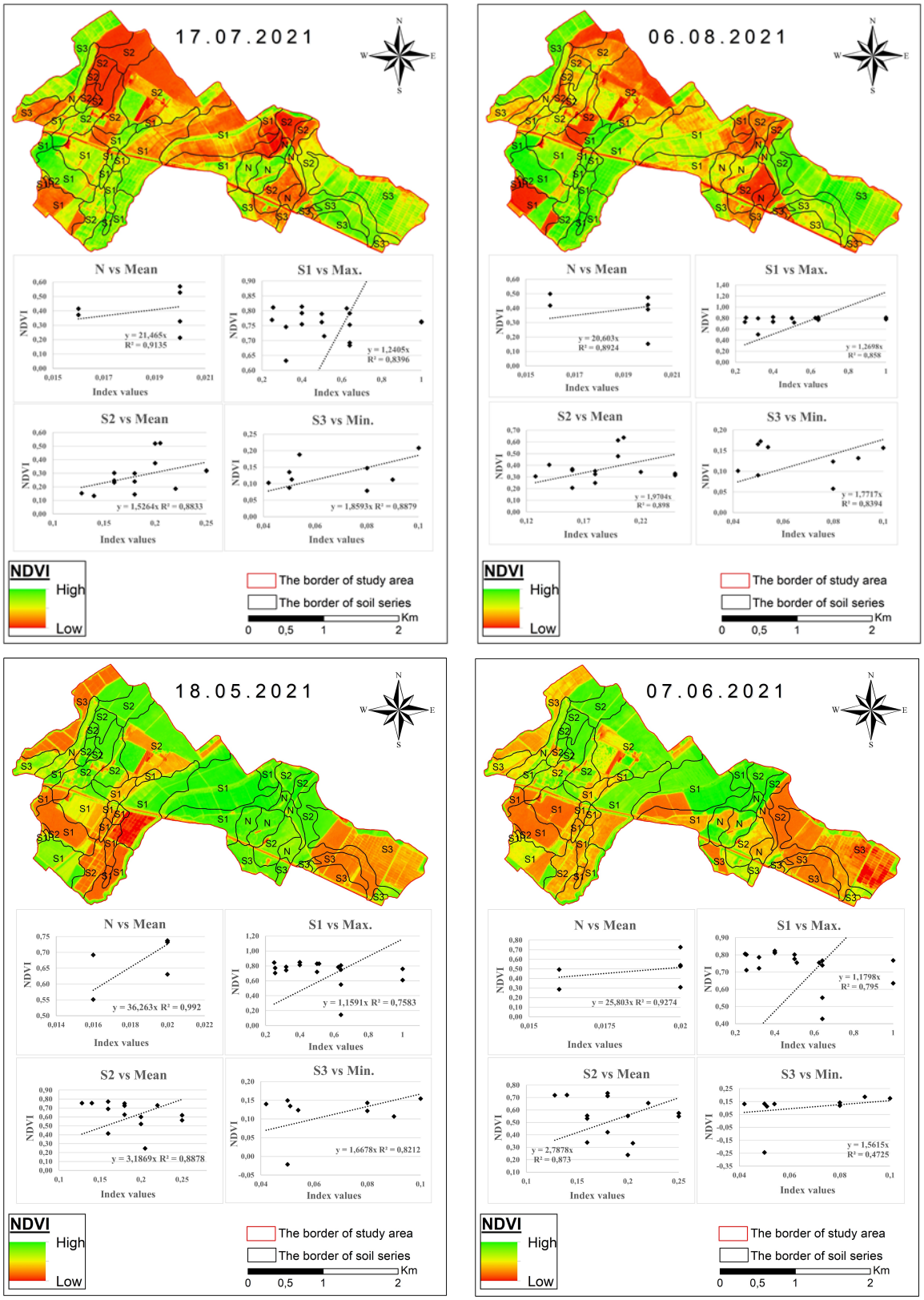

Figure 6. r2 values of each land suitability index value of rice fields and NDVI values obtained from Sentinel-2A satellite images with different time series.

The r^2 values, in which the statistical relationship is established between the NDVI values obtained from the May, June, July, and August satellite images of the Yeşil Küre Farm Land Enterprise, dated 2021, without evaluating the land suitability classes (S1, S2, S3, and N) separately, are shown in

Figure 7 and Table 6, respectively. In the evaluation of the statistical relationship between the land suitability classes (S1, S2, S3, and N) and the NDVI values without evaluating them separately, the r^2 values for July and August, which were determined to be high, were determined as 0.5707 and 0.6321, respectively, according to the r^2 results discussed. According to the r^2 results, which were considered in the evaluation of the statistical relationship between the NDVI values without evaluating the land suitability classes (S1, S2, S3, and N) separately, the r^2 values for the months of May and June, which were determined as low, were determined as 0.3341 and 0.4297, respectively.

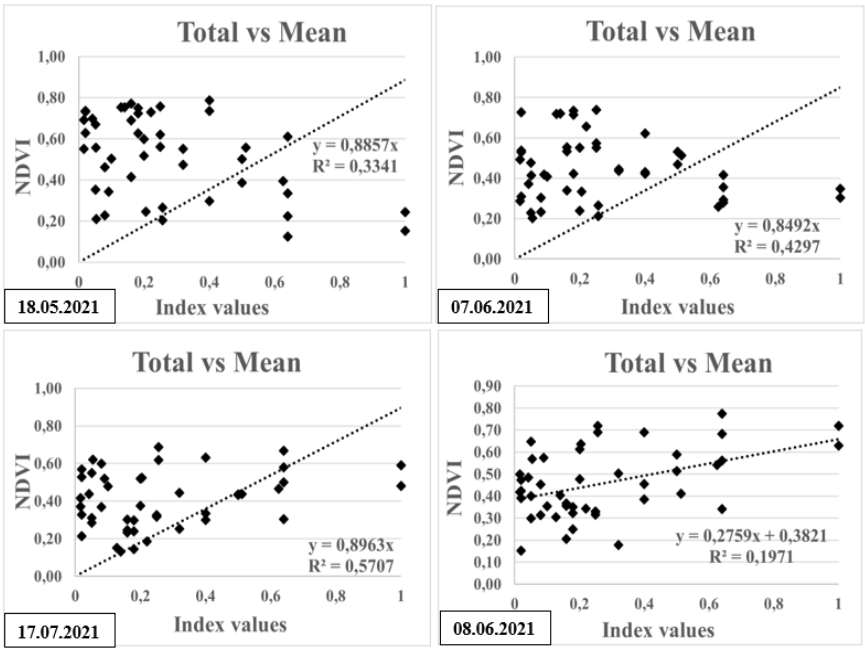

Figure 7. Land suitability index values of rice fields and r^2 values of NDVI values obtained from Sentinel-2A satellite images with different time series.

The highest r^2 values for NDVI were obtained in satellite images of July and August. This situation was associated with the fact that the plant vegetation density of the rice fields reached its maximum value within a month from mid-July. The high NDVI values of the July and August satellite images may also be associated with the shade forming feature of the rice plant (structural or vegetation cover percentage). The abundance of the stem and leaves of the rice plant reduces the reflectance effects of the plant substrate, and thus the enhanced vegetation of the rice allows more reliable estimates of the NDVI reflectance values, an index based on slope (Panda et al., 2010; Mirasi et al., 2019). As a matter of fact, Verhulst et al. (2009) reported that NDVI vegetation indices have a strong correlation with plant physiological parameters, crop yield and biomass.

The lowest r^2 values for NDVI were obtained in satellite images of May and June. In this period (May-June), the rice plant is in tillering period and tillering is one of the basic rice growth stages that determines the final yield. During the first six months after the start of the rice season (until the end of June), it is known that there is almost no correlation between the spectral reflectance values and the AUI values, considering the short height of the rice plant and the fact that it is a plant that grows constantly under water (Franch et al., 2021). This is considered as an important reason why the relationship between NDVI values and AUI values of satellite images in May and June is lower than in July and August.

Table 6. Land suitability index values of rice lands of Yeşil Küre Agricultural Enterprise and NDVI values of different time series satellite images

		NDVI Values			
Mapping Unit	Land Suitability Index	18.05.2021 Sentinel-2A	07.06.2021 Sentinel-2A	17.07.2021 Sentinel-2A	06.08.2021 Sentinel-2A
B11	0.02	0.6305	0.3091	0.2132	0.1530
B7	0.02	0.7319	0.5377	0.5690	0.4742
B8	0.016	0.6916	0.2862	0.4149	0.4987
B9	0.02	0.7359	0.7263	0.3275	0.3910
K11	0.016	0.5512	0.4934	0.3717	0.4185
K12	0.02	0.7368	0.5280	0.5277	0.4237
YOL	--	--	--	--	--
A1	0.4	0.8119	0.8233	0.8135	0.8203
Ba.2	0.32	0.7416	0.7217	0.6324	0.5041
Ba.4-A4	1	0.6086	0.6348	0.7634	0.8094
Ba3	0.64	0.8059	0.7391	0.6923	0.7842
E2	0.64	0.5477	0.5507	0.6835	0.7711
E4-Y3	1	0.7583	0.7677	0.7614	0.7795
E5	0.64	0.7501	0.7662	0.7530	0.7753
K10	0.256	0.7043	0.7114	0.8114	0.8093
K3	0.256	0.7723	0.8009	0.8109	0.8050
K3	0.625	0.7828	0.7541	0.8081	0.8037
K6	0.4	0.8459	0.8108	0.7922	0.7317
K7	0.32	0.7860	0.7860	0.7455	0.7968
K8	0.5	0.7195	0.7766	0.7615	0.7950
K8	0.5	0.8282	0.8011	0.7897	0.8043
K9	0.512	0.8277	0.7542	0.7146	0.7198
Y1-E1	0.25	0.8435	0.8053	0.7691	0.7305
Y2	0.4	0.8481	0.8136	0.7547	0.7351
Y4-A3	0.205	0.2462	0.3331	0.5227	0.6367
Y5	0.16	0.4133	0.3386	0.2319	0.2064
A2	0.18	0.6273	0.4220	0.2983	0.2493
A4	0.2	0.5202	0.2388	0.5191	0.6134
A4	0.16	0.7707	0.5536	0.2460	0.3673
A4	0.18	0.7244	0.7342	0.2395	0.3238
B10	0.22	0.7302	0.6552	0.1863	0.3435
B5-B9	0.16	0.6897	0.5321	0.3012	0.3566
B6	0.25	0.6195	0.5511	0.3192	0.3295
Ba.1	0.18	0.7500	0.7136	0.1442	0.3505
Ba.4-A4	0.2	0.5989	0.5520	0.3741	0.4768
E3	0.14	0.7540	0.7198	0.1325	0.4039
E3	0.25	0.5630	0.5738	0.3178	0.3148
K2	0.128	0.7534	0.7182	0.1519	0.3046
K2	0.1	0.1545	0.1746	0.2079	0.1565
K2	0.08	0.1216	0.1179	0.0786	0.0579
B1	0.08	0.1430	0.1403	0.1470	0.1236
B2	0.054	0.1237	0.1312	0.1880	0.1586
B3	0.042	0.1402	0.1308	0.1027	0.1011
K1	0.05	-0.0218	-0.2451	0.1350	0.1657
O1	0.051	0.1344	0.1119	0.1129	0.1728
O	0.09	0.1067	0.1851	0.1123	0.1321
B	0.05	0.1492	0.1322	0.0876	0.0906

A*: Alaylı, B*: Kalaba, E*: Elifli, K*: Karaköy, O*: Osmanbeyli, Y*: Yörükler.

RE-OSAVI is a plant index that functions with the Red-Edge spectral reflectance band, which is stated to be able to reduce the spectral reflectance values of plants and the substrate reflection effects (Feng et al., 2014), and has a widespread and reliable use in the determination of plant biomass (Fitzgerald et al. et al., 2010). There is a strong correlation between RE-OSAVI and plant chlorophyll content, and the RE-OSAVI index is used in plant yield potential estimation studies (Huang et al., 2017).

The land suitability index values for each land suitability class (S1, S2, S3, and N) of the rice fields obtained from the satellite images of May, June, July, and August dated May, June, July, and August 2021 of Yeşil Küre Agricultural Enterprise and different time series Sentinel-2A satellite images were obtained. The RE-OSAVI values obtained and the r^2 values with which the statistical relationship was established are given in Table 7 and Figure 8, respectively. When the statistical relationship between the RE-OSAVI values obtained from the satellite image of May and the rice suitability index classes (S1, S2, S3, and N) was examined, the r^2 values were found to be 0.7167, 0.9135, 0.0265 and 0.9877, respectively, while the RE-OSAVI values obtained from the satellite image of June were examined. - The r^2 values determined as a result of the statistical relationship between the OSAVI values and the

rice suitability index classes (S1, S2, S3, and N) were determined to be 0.795, 0.873, 0.4725, and 0.9274, respectively.

In addition, the r^2 values obtained as a result of the statistical relationship between the RE-OSAVI values obtained from the satellite image of July and the rice suitability index classes (S1, S2, S3, and N) were 0.8465, 0.915, 0.789, and 0.8872, respectively. When the statistical relationship between the RE-OSAVI values obtained from the satellite image of the rice plant and the rice suitability index classes (S1, S2, S3, and N) was examined, the r^2 values were determined as 0.8162, 0.8907, 0.7987 and 0.9166, respectively.

Table 7. Each land suitability index values of rice fields and RE-OSAVI values of Sentinel-2A satellite images with different time series

Mapping Unit	Land Suitability Index	Land Suitability Class	RE-OSAVI Values			
			18.05.2021 Sentinel-2A	07.06.2021 Sentinel-2A	17.07.2021 Sentinel-2A	06.08.2021 Sentinel-2A
B11	0.02	N	0.5221	0.2285	0.1982	0.1449
B7	0.02	N	0.6483	0.4863	0.5277	0.4361
B8	0.016	N	0.6105	0.2657	0.3853	0.4832
B9	0.02	N	0.6705	0.6843	0.3060	0.3644
K11	0.016	N	0.4682	0.3984	0.3331	0.3746
K12	0.02	N	0.6448	0.4629	0.4619	0.3645
YOL	--	--	--	--	--	--
A1	0.4	S1	0.7384	0.7729	0.7637	0.8375
Ba.2	0.32	S1	0.6684	0.6188	0.6092	0.4404
Ba.4-A4	1	S1	0.5071	0.5591	0.7191	0.8104
Ba3	0.64	S1	0.7445	0.6640	0.6096	0.8017
E2	0.64	S1	0.4385	0.4156	0.5915	0.7111
E4-Y3	1	S1	0.5760	0.6352	0.6285	0.7441
E5	0.64	S1	0.5945	0.6507	0.6071	0.7379
K10	0.256	S1	0.6130	0.5823	0.7785	0.8278
K3	0.256	S1	0.7377	0.7229	0.7868	0.8221
K3	0.625	S1	0.7234	0.6704	0.7734	0.8124
K6	0.4	S1	0.8327	0.7623	0.7033	0.7180
K7	0.32	S1	0.6841	0.7069	0.7229	0.8297
K8	0.5	S1	0.5838	0.7057	0.7466	0.8138
K8	0.5	S1	0.8099	0.7644	0.7675	0.8231
K9	0.512	S1	0.7576	0.6745	0.6849	0.6458
Y1-E1	0.25	S1	0.8308	0.7586	0.7459	0.7176
Y2	0.4	S1	0.8379	0.7521	0.6801	0.7212
Y4-A3	0.205	S2	0.2286	0.2368	0.4463	0.5875
Y5	0.16	S2	0.3517	0.2639	0.1922	0.2002
A2	0.18	S2	0.5489	0.3448	0.2783	0.2354
A4	0.2	S2	0.4573	0.1898	0.4607	0.5657
A4	0.16	S2	0.7066	0.5228	0.2296	0.3397
A4	0.18	S2	0.6465	0.6719	0.2332	0.3003
B10	0.22	S2	0.6243	0.5178	0.1776	0.3186
B5-B9	0.16	S2	0.5771	0.4203	0.2798	0.3265
B6	0.25	S2	0.5282	0.4482	0.2896	0.3067
Ba.1	0.18	S2	0.6251	0.5459	0.1576	0.3322
Ba.4-A4	0.2	S2	0.5132	0.4543	0.3497	0.4378
E3	0.14	S2	0.6186	0.5460	0.1361	0.3606
E3	0.25	S2	0.4915	0.4749	0.2878	0.2954
K2	0.128	S2	0.6493	0.5729	0.1495	0.2804
K2	0.1	S3	0.1098	0.1679	0.1781	0.1727
K2	0.08	S3	-0.0444	0.1081	0.1303	0.1106
B1	0.08	S3	0.1252	0.1149	0.1291	0.1524
B2	0.054	S3	-0.0394	-0.0505	0.1930	0.1510
B3	0.042	S3	0.1322	0.0605	0.0972	0.1057
K1	0.05	S3	-0.0917	-0.3849	0.0779	0.1583
O1	0.051	S3	0.0991	0.0773	0.1214	0.1965
O2	0.09	S3	0.0479	0.0108	0.0840	0.1268
B12	0.05	S3	0.1393	0.1171	0.0863	0.0803

A*: Alaylı, B*: Kalaba, E*: Elifli, K*: Karaköy, O*: Osmanbeyli, Y*: Yörükler.

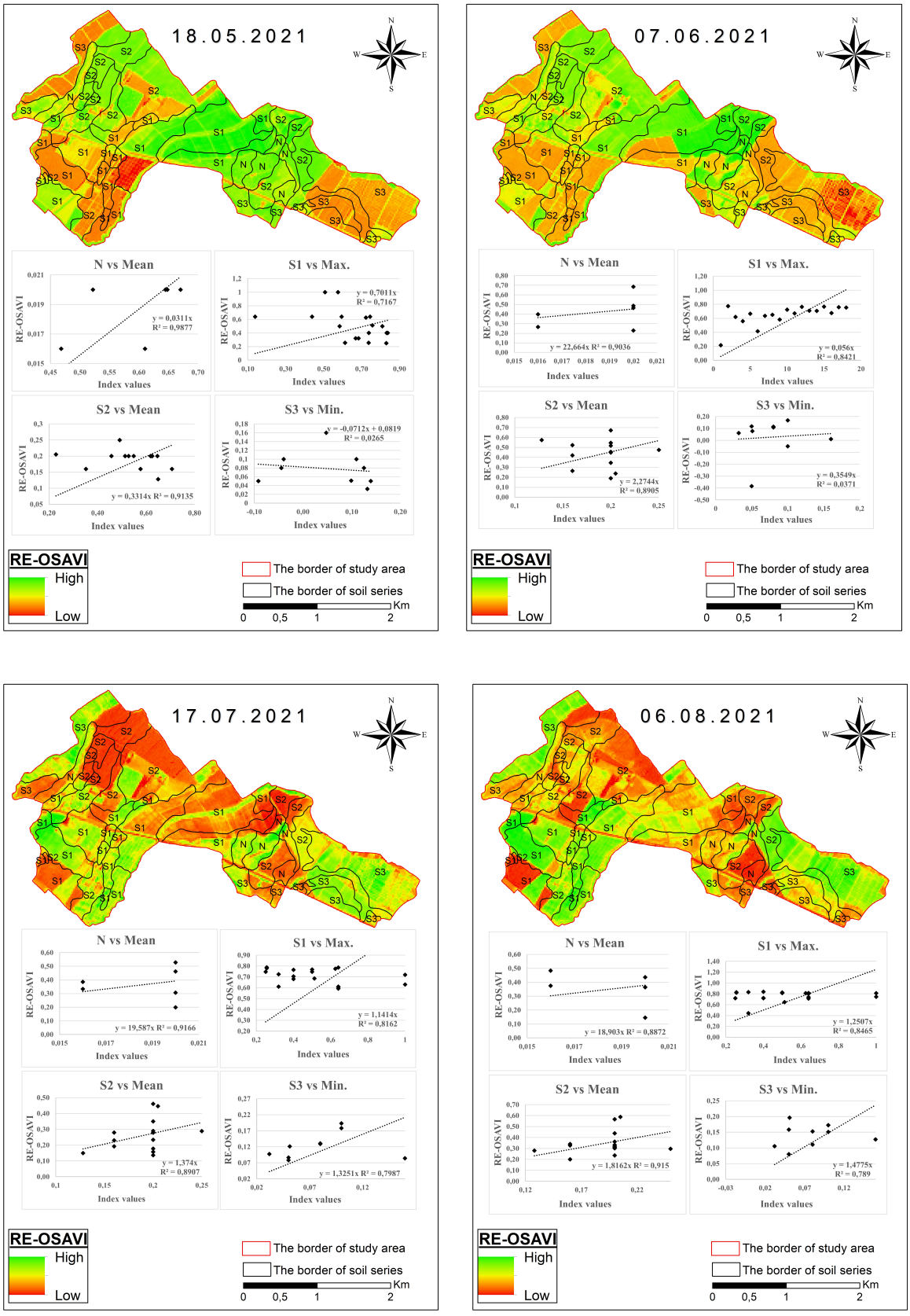

Figure 8. The r^2 values of each land suitability index value of rice fields and RE-OSAVI values obtained from Sentinel-2A satellite images with different time series.

It is thought that the low results of RE-OSAVI values in May and June are due to the fact that this index was calculated to represent the soil series instead of establishing a relationship with the rice land suitability index values. It is also predicted that the effects of climatic and atmospheric conditions may have reduced the vegetation index prediction values. Such problems show the fragile side of using remote sensing for agricultural purposes, especially when the database is limited. For this reason, it is predicted that in future similar studies with spectral vegetation indices, more successful results will be obtained when soil series and reference plant plots of similar size are used (Dedeoğlu et al., 2020).

The r^2 values, in which the statistical relationship is established between the RE-OSAVI values obtained from the satellite images of May, June, July, and August of 2021 dated May, June, July, and August belonging to the Yeşil Küre Farm Land and the land suitability classes (S1, S2, S3, and N) without evaluating them separately, are shown in Figure 9, respectively, and are given in Table 8. According to the r^2 results considered in the statistical evaluation between the RE-OSAVI values without evaluating the land suitability classes separately, the relationship between the RE-OSAVI values obtained from the satellite images of July and August, which were determined to be high, and the suitability index classes (S1, S2, S3, and N). The r^2 values were determined as 0.5732 and 0.6508, respectively. According to the r^2 results, in which the statistical relationship between the land suitability classes (S1, S2, S3, and N) and the RE-OSAVI values was evaluated without evaluating them separately, the r^2 values for the months of May and June, which were determined to be low, were determined as 0.3433 and 0.4012, respectively. According to these results, it was seen that the use of RE-OSAVI index of rice plants in late vegetation periods is suitable for estimating soil fertility potential, but not in early vegetation periods.

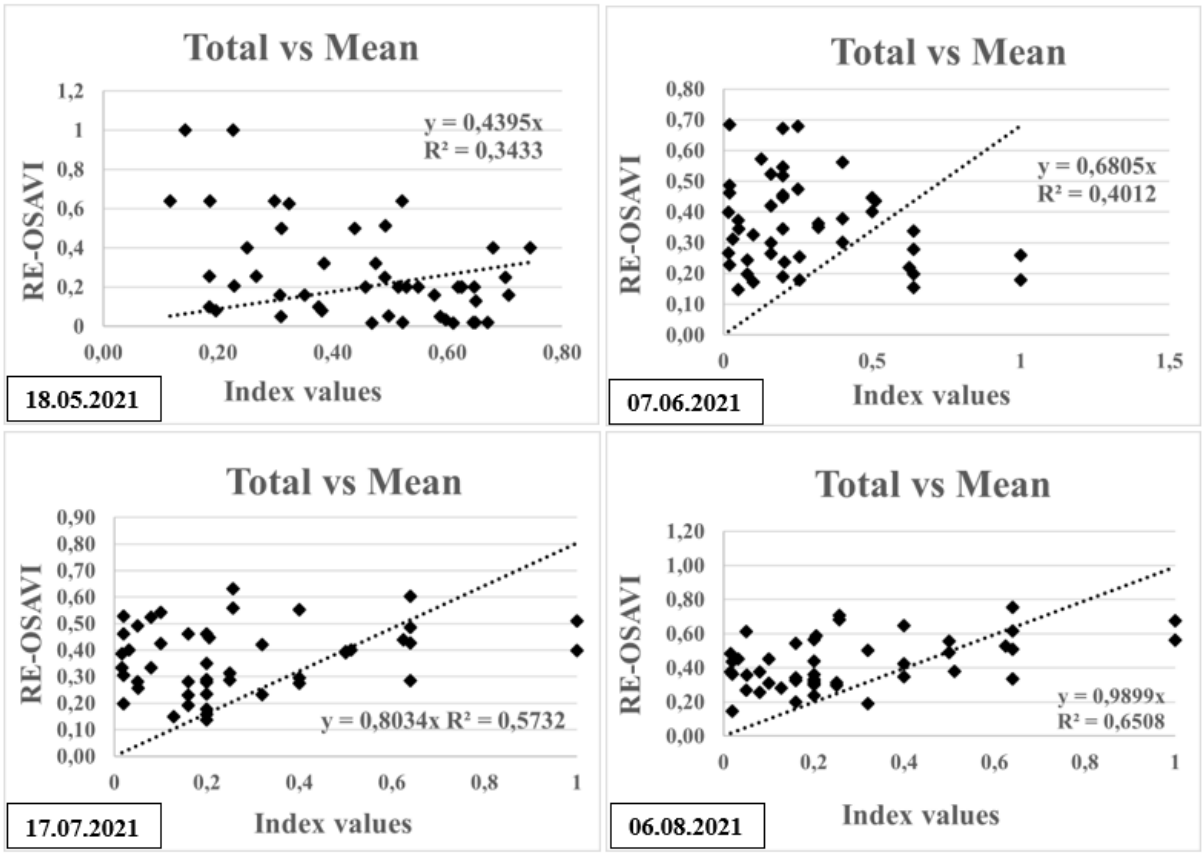

Figure 9. Land suitability index values of rice fields and r^2 values of RE-OSAVI values obtained from Sentinel-2A satellite images with different time series

Table 8. Land suitability index values of rice fields and RE-OSAVI values of different time series satellite images

Mapping Unit	Land Suitability Index	RE-OSAVI Values			
		18.05.2021 Sentinel-2A	07.06.2021 Sentinel-2A	17.07.2021 Sentinel-2A	06.08.2021 Sentinel-2A
B11	0.02	0.5221	0.2285	0.1982	0.1449
B7	0.02	0.6483	0.4863	0.5277	0.4361
B8	0.016	0.6105	0.2657	0.3853	0.4832
B9	0.02	0.6705	0.6843	0.3060	0.3644
K11	0.016	0.4682	0.3984	0.3331	0.3746
K12	0.02	0.6448	0.4629	0.4619	0.3645
YOL	0.64	0.1168	0.1538	0.6020	0.7552
YOL-A1	0.4	0.2509	0.3008	0.5523	0.6456
Ba.2	0.32	0.4750	0.3618	0.2315	0.1909
Ba.4-A4-Ba	1	0.1422	0.1780	0.5091	0.6747
Ba3	0.64	0.5209	0.3372	0.2846	0.3347
E2	0.64	0.1858	0.1985	0.4855	0.6155
E4-Y3	1	0.2269	0.2587	0.3978	0.5633
E5	0.64	0.2985	0.2786	0.4270	0.5084
K10	0.256	0.1849	0.1792	0.5578	0.6803
K3	0.256	0.2660	0.2547	0.6306	0.7064
K3	0.625	0.3239	0.2196	0.4388	0.5260
K6	0.4	0.6785	0.3789	0.2955	0.3482
K7	0.32	0.3849	0.3495	0.4209	0.5028
K8	0.5	0.3114	0.4007	0.3946	0.4903
K8	0.5	0.4389	0.4463	0.3908	0.5557
K9	0.512	0.4920	0.4367	0.3999	0.3794
Y1-E1	0.25	0.7007	0.6792	0.3129	0.3143
Y2	0.4	0.7449	0.5619	0.2740	0.4230
Y4-A3	0.205	0.2286	0.2368	0.4463	0.5875
Y5	0.16	0.3517	0.2639	0.1922	0.2002
A2	0.18	0.5489	0.3448	0.2783	0.2354
A4	0.2	0.4573	0.1898	0.4607	0.5657
A4	0.16	0.7066	0.5228	0.2296	0.3397
A4	0.18	0.6465	0.6719	0.2332	0.3003
B10	0.22	0.6243	0.5178	0.1776	0.3186
B5-B9	0.16	0.5771	0.4203	0.2798	0.3265
B6	0.25	0.5282	0.4482	0.2896	0.3067
Ba.1	0.18	0.6251	0.5459	0.1576	0.3322
Ba.4-A4-Ba	0.2	0.5132	0.4543	0.3497	0.4378
E3	0.14	0.6186	0.5460	0.1361	0.3606
E3	0.25	0.4915	0.4749	0.2878	0.2954
K2	0.128	0.6493	0.5729	0.1495	0.2804
K2	0.1	0.3755	0.3254	0.4239	0.3101
K2	0.08	0.1964	0.1973	0.5238	0.3752
B1	0.08	0.3802	0.2426	0.3338	0.2559
B2	0.054	0.1853	0.1723	0.5429	0.4509
B3	0.042	0.5964	0.3112	0.4003	0.4499
K1	0.05	0.3103	0.1475	0.4905	0.6109
O1	0.051	0.4975	0.3452	0.2557	0.3566
O	0.09	0.3069	0.2999	0.4610	0.5423
B	0.05	0.5876	0.3734	0.2812	0.2685

A*: Alaylı, B*: Kalaba, E*: Elifli, K*: Karaköy, O*: Osmanbeyli, Y*: Yörükler.

Conclusion

In this study, the statistical relationship between the land suitability indices determined for rice lands belonging to Yeşil Küre Agricultural Enterprise and the spectral vegetation index (NDVI and RE-OSAVI) values calculated by using different time series Sentinel-2A satellite images, and the estimation of the rice productivity potential. A different perspective is presented for viewing and monitoring. First of all, according to the rice conformity assessment study of the farm lands, 6488.9 ha area was determined to be suitable for rice cultivation at S1 and S2 levels, while the 588.9 ha area was determined to be unsuitable. In this study, it was observed that the most successful results for each land suitability class were obtained by using the NDVI index. It has been determined that the RE-OSAVI index gives more accurate results in determining the sparse vegetation, and provides a limited opportunity to monitor cultivars grown in water-saturated land conditions.

The r^2 values, in which the statistical relationship between the rice land suitability index values values were revealed without evaluating the land suitability classes separately, showed that both indices

were not suitable for soil fertility potential estimations in early vegetation periods, but were suitable for soil fertility potential estimations in medium to long vegetation periods. It was concluded that the vegetation indices obtained from the satellite images of the different growth stages of the rice plant can be used as an alternative to determine the critical growth stages of the rice plant. With this study, it is predicted that the use of vegetation indices can help to monitor the rice plant at critical time stages and to intervene in time to possible problems, as well as to ensure the continuity of food safety by getting more yield from the rice plant with these interventions. In addition, this study showed that the spectral capabilities of Sentinel-2A satellite images can be used in similar studies to be done in the future with the ESA-SNAP image processing tool. As a result, this study using vegetation index values obtained from different time series satellite images covering different development stages of rice plants has created an awareness for future research in determining the potentials for the relationships between index values and rice soil quality.

References

Ahmed, G. B., Shariff, A.R.M., Balasundram, S.K., & Fikri bin Abdullah, A. (2016). Agriculture land suitability analysis evaluation based multi criteria and GIS approach. IOP Conference series: *Earth and Environmental Science*, 37, 012044.

Al-Bakri, J.T., & Suleiman, A.S. (2004). NDVI response to rainfall in different ecological zones in Jordan. *International Journal of Remote Sensing*, 25(19), 3897-3912.

Askari, M.S., Cui, J., O'Rourke, S.M., & Holden, N.M. (2015). Evaluation of soil structural quality using VIS–NIR spectra. Soil and Tillage Research, 146, 108–117.

Bagheri, N., Ahmadi, H., Alavipanah, S., & Omid, M. (2012). Soil-line vegetation indices for corn nitrogen content prediction. *International Agrophysics*, 26(2), 103–108.

Barnes, E., Clarke, T., Richards, S., Colaizzi, P., Haberland, J., Kostrzewski, M., Waller, P., Choi, C., Riley, E., Thompson, T., Lascano, R. J., Li, H., & Moran, M.S. (2000). *Coincident detection of crop water stress, nitrogen status and canopy density using ground based multispectral data*. In Proceedings of the Fifth International Conference on Precision Agriculture, Bloomington, MN, USA, 2000 (Vol. 1619).

Blum, W.E.H. (2006). *Soil Resources- The basis of human society and the environment*. Bodenkultur 57, 197–202.

Damian, J.M., Pias, O.H.D.C., Cherubin, M.R., Fonseca, A.Z.D., Fornari, E.Z., Santi, A.L., (2020). Applying the NDVI from satellite images in delimiting management zones for annual crops. *Sci. Agric*. 77 (1).

Dedeoğlu, M., Başayiğit, L., Yüksel, M., & Kaya, F. (2020). Assessment of the vegetation indices on Sentinel-2A images for predicting the soil productivity potential in Bursa, Turkey. *Environmental Monitoring and Assessment*, 192(1), 1-16.

Demir, S., & Başayiğit, L. (2021). Kısıtlı sulama uygulamalarının İHA multispektral algılamaya dayalı vejetasyon indekslerine etkisi. *Yuzuncu Yıl University Journal of Agricultural Sciences*, 31(3), 629-643.

Dengiz, O. (2013). Land suitability assessment for rice cultivation based on GIS modeling. *Turkish Journal of Agriculture and Forestry*. 37: 326-334, DOI: 10.3906/tar-1204-36.

Dengiz, O. (2020). Soil quality ındex for paddy fields based on standard scoring functions and weight allocation method. *Archives of Agronomy and Soil Science*, 66(3), 301-315.

Dengiz, O., & Sağlam, M. (2012). Determination of land productivity index based on parametric approach using GIS technique. *Eurasian Journal of Soil Science*, 1, 51–57.

Doran, J.W., & Parkin, T.B. (1994). *Defining and assessing soil quality*. Defining soil quality for a sustainable environment, 35, 1-21.

Dumanski, J., & Peiretti, R. (2013). Modern concepts of soil conservation. *International soil and water conservation research*, 1(1), 19-23.

Explorer, E. (2000). *Geological Survey* (US). Earth observatory NASA. http://earthobservatory.nasa.gov/Features/MeasuringVegetation.

ESRI, (2010). *ArcGIS user's guide*. http://www.esri.com

FAO, (1983). *Land and Water Development Division. Guidelines: land evaluation for rainfed agriculture*. Food and Agriculture Organization of the United Nations.

FAO (1985). *Guideline: land evaluation for irrigated agriculture*. FAO Soils Bulletin, No. 55, Rome

FAO, I., & ISRIC, I. (2009). *Harmonized world soil database (version 1.1)*. FAO, Rome, Italy and IIASA, Laxenburg, Austria. http://www.fao.org/nr/land/soils/harmonized-world-soildatabase/en.

Feng, W., Guo, B.-B., Wang, Z. J., He, L., Song, X., Wang, Y. H., & Guo, T.C. (2014). Measuring leaf nitrogen concentration in winter wheat using double-peak spectral reflection remote sensing data. *Field Crops Research*, 159: 43–52.

Fitzgerald, G., Rodriguez, D., & O'Leary, G. (2010). Measuring and predicting canopy nitrogen nutrition in wheat using a spectral index—the canopy chlorophyll content index (CCCI). *Field Crops Research*, 116(3), 318–324.

Franch, B., Bautista, A.S., Fita, D., Rubio, C., Tarrazó-Serrano, D., Sánchez, A., Skakun, S., Vermote, E., Becker-Reshef, I., & Uris, A. (2021). Within-Field Rice Yield Estimation Based on Sentinel-2 Satellite Data. *Remote Sensing*, 13(20), 4095.

Gupta, R.K., Vijayan, D., & Prasad, T.S. (2003). Comparative analysis of red-edge hyperspectral indices. *Advances in Space Research*, 32(11), 2217–2222.

Huang, S., Miao, Y., Yuan, F., Gnyp, M., Yao, Y., Cao, Q., Wang, H., Lenz-Wiedemann, V., & Bareth, G. (2017). Potential of RapidEye and WorldView-2 satellite data for improving rice nitrogen status monitoring at different growth stages. *Remote Sensing*, 9(3), 227.

Hufkens K., Melaas, E.K., Foster, T., Ceballos, F., Robles, M., & Kramer, B. (2019). Monitoring crop phenology using a smartphone based near-surface remote sensing approach. *Agricultural and Forest Meteorology*, 265: 327-337.

Jackson, R.D. (1986). Remote sensing of biotic and abiotic plant stress. *Annual Review of Phytopathology*, 24(1), 265–287.

Jia, L., Yu, Z., Li, F., Gnyp, M., Koppe, W., Bareth, G., Miao, Y., Chen, X., & Zhang, F. (2011). Nitrogen status estimation of winter wheat by using an Ikonos satellite image in the north china plain. *Computer and computing technologis in agriculture V. 5th IFIP TC5/SIG 5,1 Conference*, CCTA 2011 Beijing, Cina, October 2011 Proceedings, Part II.

Jiang, L., Liu, Y., Wu, S., & Yang, C. (2021). Analyzing ecological environment change and associated driving factors in China based on NDVI time series data. *Ecological Indicators*, 129: 107933.

Jones, A., Stolbovoy, V., Rusco, E., Gentile, A.R., Gardi, C., Marechal, B., & Montanarella, L. (2009). Climate change in Europe. 2. Impact on soil. A review. *Agronomy for sustainable development*, 29(3), 423-432.

Karlen D.L., Mausbach M.J., Doran J.W., Cline R.G., Harris R.F., & Schuman G.E. (1997). Soil quality: a concept, definition and framework for evaluation. *Soil Sci. Soc. Am. J.* 61, 4–10.

Kerr, J.T., & Ostrovsky, M. (2003). From space to species: ecological applications for remote sensing. *Trends in ecology & evolution*, 18(6), 299-305.

Kokaly, R.F., & Clark, R.N. (1999). Spectroscopic determination of leaf biochemistry using band-depth analysis of absorption features and stepwise multiple linear regression. *Remote Sensing of Environment*, 67(3), 267–287.

Kostrzewski, M., Waller, P., Guertin, P., Haberland, J., Colaizzi, P., Barnes, E., Thompson, T., Clarke, T., Riley, E., & Choi, C. (2003). Ground-based remote sensing of water and nitrogen stress. *Transactions of the ASAE*, 46(1), 29.

Lal R. (2008). *Soils and sustainable agriculture*. A review, Agron. Sustain. Dev. 28, 57–64.

Lal R. (2009). *Soils and food sufficiency*. A review, *Agron. Sustain. Dev*. 29, 113–133.

Larson, W. E., & Pierce, F. J. (1991). *Conservation and enhancement of soil quality*. In Evaluation for sustainable land management in the developing world: Proceedings of the International Workshop on Evaluation for Sustainable Land Management in the Developing World, Chiang Rai, Thailand, 15-21 September 1991.

Lichtfouse, E., Navarrete, M., Debaeke, P., Souchère, V., & Alberola, C. (2009). *Sustainable Agriculture*. Springer, 1st ed., 645 p., ISBN: 978-90-481-2665-1.

Liniger, H.P., Studer, R.M., Hauert, C., & Gurtner, M. (2011). Sustainable land management in practice: guidelines and best practices for Sub-Saharan Africa. *FAO*.

Liu, J., Miller, J. R., Haboudane, D., & Pattey, E. (2004). *Exploring the relationship between red edge parameters and crop variables for precision agriculture*. IEEE International Geoscience and Remote Sensing Symposium (Vol. 2, pp. 1276-1279).

Malczewski, J. (2006). Ordered weighted averaging with fuzzy quantifiers: GIS-based multicriteria evaluation for land-use suitability analysis. *International Journal of Applied Earth Observation and Geoinformation*, 8(4), 270–277.

Matton, N., Canto, G.S., Waldner, F., Valero, S., Morin, D., Inglada, J., Arias, M., Bontemps, S., Koetz, B., & Defourny, P. (2015). An automated method for annual cropland mapping along the season for various globally distributed agrosystems using high spatial and temporal resolution time series. *Remote Sensing*, 7(10): 13208-13232.

Mezera, J., Lukas, V., & Elbl, J. (2017). Evaluation of crop yield spatial variability in relation to variable rate application of fertilizers. *MendelNet*, 24(1), 2017.000.

Mirasi, A., Mahmoudi, A., Navid, H., Valizadeh Kamran, K., & Asoodar, M.A. (2019). Evaluation of sum-NDVI values to estimate wheat grain yields using multi-temporal Landsat OLI data. *Geocarto International*, 36(12), 1309–1324.

Mongkolsawat, C.P., Thirangoon, & Kuptawutinan, P. (2002). *A physical evaluation of landsuitability for rice: A methodological study using GIS*. Computer Centre, Khon Kaen University, Thailand. http://www. gisdevelopment.net.

Moran, M.S., Rahman, A.F., Washburne, J.C., Goodrich, D.C., Weltz, M.A., & Kustas, W.P. (1996). Combining the Penman-Monteith equation with measurements of surface temperature and reflectance to estimate evaporation rates of semiarid grassland. *Agricultural and Forest Meteorology*, 80(2), 87–109.

MTA, (1974). *1:500000 scaled Geological Map of Turkey*. General Directorate of Maps Printing House, 1974, Ankara.

Mueller, L., Schindler, U., Mirschel, W., Shepherd, T.G., Ball, B.C., Helming, K., Rogasik J., Eulenstein F., & Wiggering H. (2010). Assessing the productivity function of soils. *In Sustainable Agriculture*, 2:743– 760.

Özbek, H., Dinç, U., & Kapur, S. (1974). *Detailed Survey and Mapping of Çukurova University Settlement Area Soils*. Ankara University Press, Ankara.

Özcan, H. (2004). *The Effect of Zinc Application on Yield and Zinc, Phosphorus and Phytin Acid Concentration in Some Rice Varieties*. A.U. Natural Science Ins., Soil Department, *from PhD thesis*, Ankara.

Panda, S.S., Ames, D.P., & Panigrahi, S. (2010). Application of vegetation indices for agricultural crop yield prediction using neural network techniques. *Remote Sensing*, 2(3), 673–696.

Pettorelli, N., Vik, J.O., Mysterud, A., Gaillard, J.M., Tucker, C.J., & Stenseth, N.C. (2005). Using the satellite-derived NDVI to assess ecological responses to environmental change. *Trends in Ecology & Evolution*, 20(9), 503-510.

Pradipta, D., (2012). *Analisis Data Time Series NDVI-SPOT Vegetation Untuk Tanaman Padi* (Studi Kasus: Kabupaten Karawang). Institut Pertanian Bogor.

Rogowski, A., & Wolf, J. (1994). Incorporating variability into soil map unit delineations. *Soil Science Society of America Journal*, 58(1), 163–174.

Rondeaux, G., Steven, M., & Baret, F. (1996). Optimization of soil-adjusted vegetation indices. *Remote Sensing of Environment*, 55(2), 95–107.

Sahararini, A.F., & Wibowo, A. (2020). *Estimation of rice productivity using Sentinel-2 imagery with NDVI algorithm in Cariu sub-district, Bogor, West Java*. In IOP Conference Series: Earth and Environmental Science (Vol. 481, No. 1, p. 012056). IOP Publishing.

Salinas-Zavala, C.A., Douglas, A.V., & Diaz, H.F. (2002). Interannual variability of NDVI in northwest Mexico. Associated climatic mechanisms and ecological implications. *Remote Sensing of Environment*, 82(2-3), 417-430.

Savaslı, E., Önder, O., Dayıoğlu, R., Didem, Ö., Karaduman, Y., Özdemir, S., & Özsayın, M. (2021). Ekmeklik Buğdayda Optik Sensör ile Azotlu Gübre Tavsiyesi. *Yuzuncu Yıl University Journal of Agricultural Sciences*, 31(2), 453-465.

Sharabıanı, V.R., Nazarloo, A.S., & Taghınezhad, E. (2019). Prediction of protein content of winter wheat by canopy of near infrared spectroscopy (NIRS), using partial least squares regression (PLSR) and artificial neural network (ANN) models. *Yüzüncü Yıl Üniversitesi Tarım Bilimleri Dergisi*, 29(1), 43-51.

Shou, L., Jia, L., Cui, Z., Chen, X., & Zhang, F. (2007). Using high-resolution satellite imaging to evaluate nitrogen status of winter wheat. *Journal of Plant Nutrition*, 30(10), 1669– 1680.

Soil Survey Staff, (1962). *Soil Survey Manuel*. Agriculture Handbook No:18. Washington D.C.

Sönmez, B. (2003). *Türkiye Çoraklık Kontrol Rehberi*. T.C Tarım ve Köyişleri Bakanlığı Köy Hizmetleri Genel Müdürlüğü, Toptak ve Gübre Araştırma Enstitüsü. Teknik Yayın No: 33.

Sys. C., Ranst, V., Debaveye, J., & Beernaert, F. (1993). *Land Evaluation Part III, Crop Requirements*. Agr. Publication No. 7, ITC Ghent.

Verhulst, N., Govaerts, B., Sayre, K. D., Deckers, J., François, I. M., & Dendooven, L. (2009). Using NDVI and soil quality analysis to assess influence of agronomic management on within-plot spatial variability and factors limiting production. *Plant and Soil*, 317(1), 41–59.

Vohland, M., Ludwig, M., Thiele-Bruhn, S., & Ludwig, B. (2014). Determination of soil properties with visible to near- and mid-infrared spectroscopy: effects of spectral variable selection. *Geoderma*, 223-225: 88–96.

Vorobiova, N., & Chernov, A. (2017). Curve fitting of MODIS NDVI time series in the task of early crops identification by satellite images. *Procedia Engineering*, 201: 184-195.

Walter, C., & Stützel, H. (2009). A new method for assessing the sustainability of land-use systems (I): Identifying the relevant issues. *Ecol. Econ*. 68, 1275–1287.

Wójtowicz, M., Wójtowicz, A., & Piekarczyk, J. (2016). Application of remote sensing methods in agriculture. *Communications in Biometry and Crop Science*, 11(1), 31– 50.

Wu, C., Niu, Z., Tang, Q., & Huang, W. (2008). Estimating chlorophyll content from hyperspectral vegetation indices: modeling and validation. *Agricultural and Forest Meteorology*, 148(8), 1230–1241.

Xue, R., Wang, C., Liu, M., Zhang, D., Li, K., & Li, N. (2019). A new method for soil health assessment based on analytic hierarchy process and meta-analysis. *Science of the Total Environment*, 650, 2771–2777.

Yamada, Y., Suzuki, M., Amorndham, W., & Sukjarn, S. (1995). Plan of the construction of GIS for northeast Thailand. *16th Asian Conference on Remote Sensing, Nakhon Ratchasima, Thailand*. (available online at http://www.a-a-r-s.org/acrs/proceeding/ ACRS1995/Papers/WSI95-4.htm).

Zand, F., & Matinfar, H.R. (2012). Winter wheat yield estimation base upon spectral data and ground measurement. *Annals of Biological Research*, 3(11), 5169–5177.

Zhou, C., Chen, S., Zhang, Y., Zhao, J., Song, D., & Liu, D. (2018). Evaluating metal effects on the reflectance spectra of plant leaves during different seasons in post-mining areas, China. *Remote Sensing*, 10(8), 1211.